Exciton Dynamics in InSb Colloidal Quantum Dots

Andrew Sills,[†] Paul Harrison,[‡] and Marco Califano[*,†]

Institute of Microwaves and Photonics, School of Electronic and Electrical Engineering, University of Leeds, Leeds LS2 9JT, United Kingdom , and Materials and Engineering Research Institute Sheffield Hallam University, Sheffield S1 1WB, United Kingdom

E-mail: m.califano@leeds.ac.uk

[*]To whom correspondence should be addressed

[†]Institute of Microwaves and Photonics, School of Electronic and Electrical Engineering, University of Leeds, Leeds LS2 9JT, United Kingdom

[‡]Materials and Engineering Research Institute Sheffield Hallam University, Sheffield S1 1WB, United Kingdom

Abstract

Extraordinarily fast biexciton decay times and unexpectedly large optical gaps are two striking features observed in InSb colloidal quantum dots that have remained so far unexplained. The former, should its origin be identified as an Auger recombination process, would have important implications regarding carrier multiplication efficiency, suggesting these nanostructures as potentially ideal active materials in photovoltaic devices. The latter could offer new insights into the factors that influence the electronic structure, and consequently the optical properties, of systems with reduced dimensionality, and provide additional means to fine tune them. Using the state-of-the-art atomistic semiempirical pseudopotential method we unveil the surprising origins of these features and show that a comprehensive explanation for these properties requires delving deep into the atomistic detail of these nanostructures and is, therefore, outside the reach of less sophisticated, albeit more popular, theoretical approaches.

Graphical TOC Entry

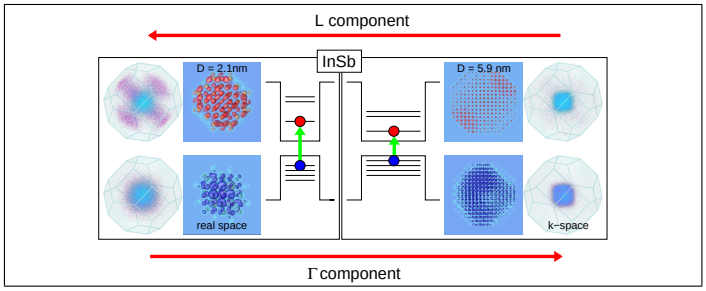

Keywords:Auger processes, nanocrystals, colloidal quantum dots, pseudopotential method, stoichiometry, k-vector analysis

Semiconductor colloidal quantum dots (CQDs) have attracted large interest due to their size tunable electronic structure and optical properties, which, when coupled with their inexpensive synthesis, make them ideal building blocks for a wide variety of optoelectronic devices. InSb CQDs are particularly promising as this material exhibits the largest electron mobility and the largest exciton Bohr radius among all bulk semiconductors,[1] combining excellent transport properties with strong confinement effects. Recent experiments have, however, evidenced peculiar optical properties[2] which still lack a satisfactory explanation. Indeed it is not clear why the band gap seems to converge to the value of the bulk band gap at L rather than to that at Γ, with increasing dot size. A possibility would be a peculiar direct-to-indirect transition taking place at a very large radius, outside the experimental range, i.e., for $R > 3.2$ nm, in contrast with what was predicted for other semiconductor materials,[3] where such a transition occurred at much smaller sizes. Furthermore the non-radiative exciton decay dynamics observed in these nanostructures still awaits theoretical elucidation. In particular, the measured biexciton recombination times,[4] attributed to Auger processes, are one order of magnitude faster in InSb CQDs than observed[5–7] and predicted[8] in materials such as CdSe, whereas the electron cooling times, also attributed to Auger decay, are in line with those commonly found in nanostructures.[5,6,8–12] These observations raise the question of whether, unlike in the case of other materials, different (intra-band and inter-band) non-radiative decay processes may be governed by different (i.e., Auger and non-Auger) mechanisms in InSb CQDs. (The unexpectedly small interlevel energy spacings within the conduction band of InSb CQDs resulting from very recent scanning tunneling spectroscopy and atomic force microscopy measurements[13] also remain unexplained. However, as the reported single-particle gaps are also found to be significantly smaller than the optical gaps measured, in the same size range, by Liu *et al.*,[2] further experimental investigation is needed

to determine the origins of this inconsistency.)

We address all these questions using a state-of-the-art atomistic semiempirical pseudopotential approach.[14] We investigate the nature of the optical transitions (i.e., direct vs indirect) by decomposing the wave functions of the conduction band edge states in terms of their k-vector components, and find that they contain sizable contributions from the high-symmetry L point in the Brillouin zone, that increase for the largest sizes considered experimentally, explaining the failure of their band edge absorption to converge to the bulk band gap at Γ. We show that this behavior is only exhibited by Sb-centered structures, highlighting the importance of the stoichiometry of the CQDs for an accurate reproduction of the experimental data, in the case of both optical spectra and population decay curves. The composition is therefore identified as a further tool to modify and fine tune the properties of InSb dots, as it has been shown to be the case for PbS nanostructures[15] Incidentally, we note that the level of accuracy required to simulate the effect of different stoichiometries is not achievable with continuum methods like the popularly adopted $\mathbf{k}\cdot\mathbf{p}$ - which cannot distinguish between the properties of In-rich/In-centered and Sb-rich/Sb-centered CQDs - but is only available to atomistic methods. In this regard, we establish the symmetry of the valence band maximum (VBM) to be s-like in both In-rich and Sb-rich CQDs within the experimental size range (i.e., transitions between band edge states are optically allowed, according to our theory), in contrast with the predictions of previous $\mathbf{k}\cdot\mathbf{p}$ calculations,[16] which found a p-type VBM, hence predicted optically forbidden band edge transitions, leading to larger band gaps. Finally, we confirm that the observed exciton decay dynamics is indeed due to Auger processes, opening the door to the exploitation of InSb CQDs in photovoltaics.

Within the semi-empirical pseudopotential approach, the CQD is built with bulk-like structure, starting from its constituent atoms, up to the desired radius. We consider both anion-centered dots (which yield Sb-rich structures for $D < 6$ nm), and cation-centered dots (resulting in In-rich stoichiometries for $D < 6$ nm[17]). This procedure yields sur-

face atoms with unsaturated bonds. Atoms with only one (saturated) bond are removed, as they are unstable for dissociation,[18] leaving on the surface only atoms with one or two missing bonds. These surface dangling bonds are passivated by pseudo-hydrogenic, short-range potentials with Gaussian form. The single-particle energies and wave functions are calculated using the plane-wave semiempirical pseudopotential method described in Reference,[14] including spin-orbit coupling, and excitonic effects are accounted for via a configuration interaction scheme.[19]

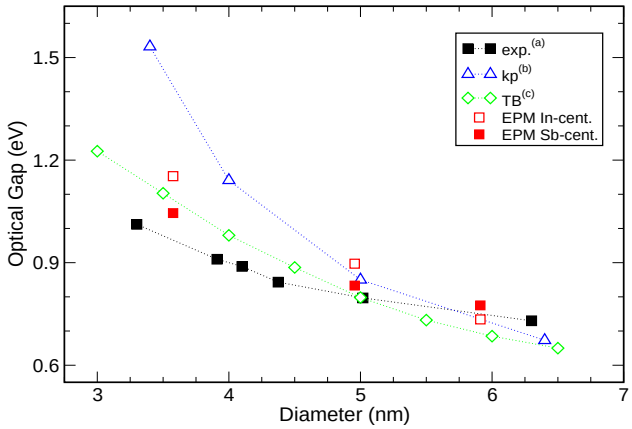

Figure 1: Optical gaps: comparison of our results (red empty squares, In-centered; red solid squares, Sb-centered) with experiment[2] (black solid squares), and the results of other theoretical approaches (8-band $\mathbf{k}\cdot\mathbf{p}$ method,[16] empty blue triangles; atomistic tight-binding approach,[20] empty green diamonds).

Auger decay times are calculated using Fermi's Golden Rule according to[8]

$$(\tau_{\mathrm{AMT}})_i^{-1} = \frac{\Gamma}{\hbar}\sum_n \frac{|<i|\Delta H|f_n>|^2}{(E_{f_n}-E_i)^2+(\Gamma/2)^2}. \tag{1}$$

where $|i>$ and $|f_n>$ are the initial and final states E_i and E_{f_n} are their energies, ΔH is the Coulomb interaction and $\hbar/\Gamma$ (in all our calculations we assume $\Gamma = 10$ meV) is the lifetime of the final states.

The Auger biexciton recombination rates τ_{XX}^{-1} are evaluated combining two contributions, τ_e^{-1} and τ_h^{-1}, deriving, respectively, from the excitation of an electron and from the

excitation of a hole as:[12]

$$\tau_{XX}^{-1} = \tau_e^{-1} + \tau_h^{-1}. \tag{2}$$

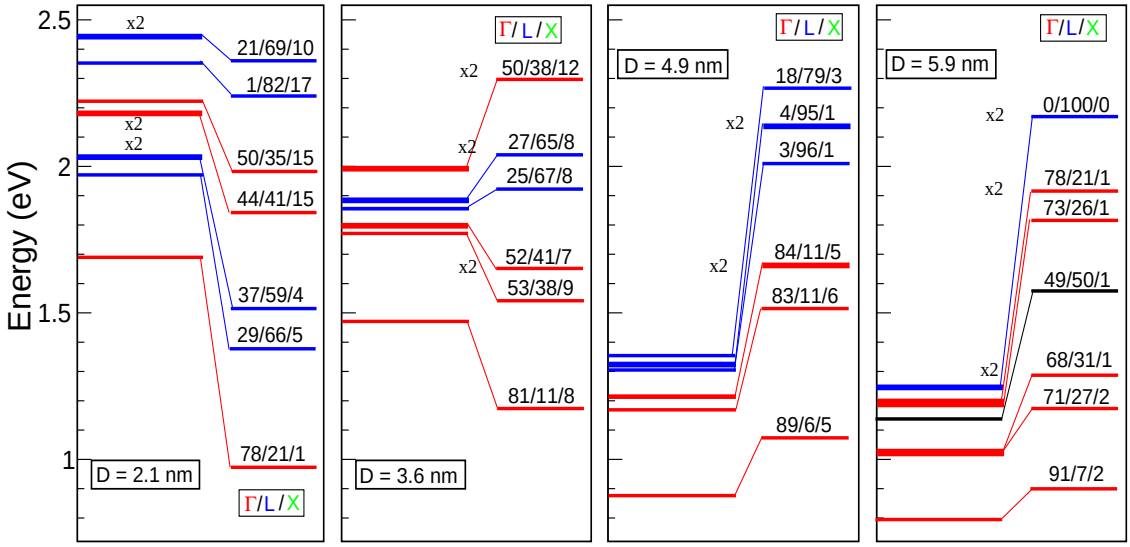

Figure 2: Conduction band electronic structure for 4 different Sb-centered dot sizes: each panel refers to a different value of the dot diameter D and displays energy levels (left-hand side) and k-vector decomposition (right-hand side). The different states are colored according to their main character (Γ red; L blue; and X green) resulting from such a decomposition. Two-fold degenerate states are indicated by '×2'.

In Figure 1, we compare the excitonic gap calculated for In-centered and Sb-centered CQDs of different sizes with the experimentally measured optical gaps.[2] It is apparent that In-rich stoichiometries yield larger gaps than observed experimentally, for small structures, whereas Sb-rich structures reproduce observation well for the range of sizes considered. Figure 1 also includes the predictions of other theoretical approaches, the continuum-like 8-band $\mathbf{k}\cdot\mathbf{p}$ method[16] and the atomistic tight-binding approach.[20] While the latter calculations (obtained for anion-centered structures) yield good agreement with experiment, the agreement achieved by the former approach is only good in a very limited size range. Most importantly, however, both theoretical curves (and our In-centered one) *cross* the experimental curve, i.e. predict an increasingly lower gap than is observed for sizes larger than about D=5 nm, a characteristic not exhibited by our Sb-centered results. As the room temperature InSb bulk band gap at Γ is 0.180 eV,[1] it would be reasonable to

expect the excitonic gap of the CQDs to converge to this value with increasing size, as the predictions of $\mathbf{k}\cdot\mathbf{p}$ theory appear to do. However, the experimental gaps seem instead to converge to a larger value, closer to the bulk band gap at L.[2] The question therefore arises of whether an indirect Γ-to-L transition is responsible for such a behavior in this size range, as already found in the case of GaAs CQDs.[3] If that were the case, since bulk InSb has a direct band gap, the conduction band of the observed dots should have a prevalent L character and should undergo an L-to-Γ transition at some large size above the experimentally explored range. In order to shed light on this interesting issue, we performed a k-space decomposition of the conduction band (CB) wave functions, following a similar procedure as in Ref.,[3] with the difference that here we use the high symmetry points Γ, L and X as seeds for a Voronoi partition of the Brillouin zone,[21] rather than using spheres centered in those points. Each of the high-symmetry points is therefore associated with a Voronoi cell in reciprocal space that has the property that each wave vector k in that cell is closer to the specific high-symmetry point than to any other.

The latter choice is preferable, as the Voronoi cells, unlike spheres, have the same symmetry as the nanostructure's first Brillouin zone, and can therefore completely fill it without overlapping.

As shown in Figure 2, the wave function of the CB edge receives a non negligible contribution from the L point in the case of small dots. Such a component decreases with increasing size, up to $D = 5$ nm and then increases again for $D = 6$ nm in Sb-centered structures, whereas in In-centered dots the L component decreases monotonically (not shown).

Interestingly we find that this trend is accompanied by a crossover between Sb-rich and In-rich structures for Sb-centered dots. In fact, for sizes smaller than $D = 6$ nm, Sb-centered nanostructures are also Sb-rich, whereas for $D = 6$ nm, the stoichiometry is slightly reversed with a less than 1% excess of In atoms.

The difference between In-centered and Sb-centered structures is apparent from Fig-

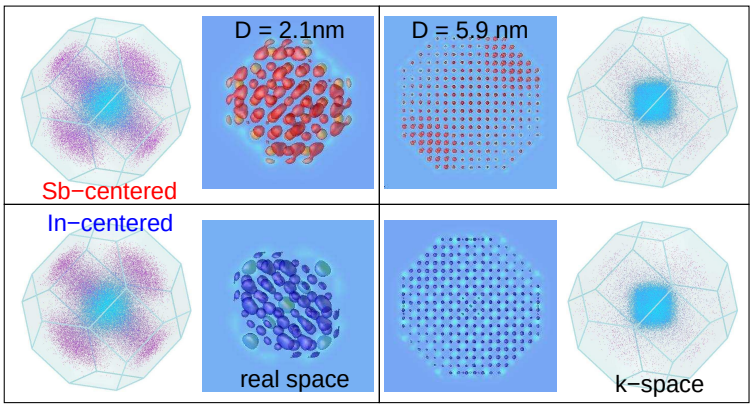

Figure 3: Real- and k-space representation of the CBM wave functions of D = 2.1 nm and 5.9 nm dots for In-centered (blue) and Sb-centered (red) structures.

ure 3, where we compare the calculated real-space and k-space representations (i.e., the charge density and the k-vector decomposition) of the CBM wave functions of the smallest and largest dot considered in our study: although the k-vector composition in In-centered and Sb-centered structures is similar for both sizes, the charge distribution is clearly different, as a result of the different stoichiometries. This is especially evident for $D = 2.1$ nm, where the relative difference in the number of atoms of the two species - 79 vs 68 - is significant. As a consequence of the mixed character of the CBM, the dot optical gap is not expected to converge to the bulk band gap at Γ for sizes within the experimental window, consistently with observation. For larger sizes the L component is expected to vanish and the gap to converge to 0.18 eV. Again it is worth stressing that the popular 8-band $\mathbf{k}\cdot\mathbf{p}$ method cannot predict this behavior, (unless new *ad-hoc* parameters are added by hand to simulate this effect *a posteriori*), and that its predicted energy gaps *underestimate* the experimental ones, for large R, despite the fact that (i) this approach is known to *overestimate* confinement (hence the band gap) due to the assumption of an infinite confining potential,[16] and (ii) its predicted *p* character for the VBM[16] would imply absorption to occur between VBM-2 and CBM, again leading to an *overestimate* of the band gap. According to our results, the VBM has instead prevalent *s*-like symmetry in both In-rich and Sb-rich CQDs within the experimental size range, and therefore transitions between

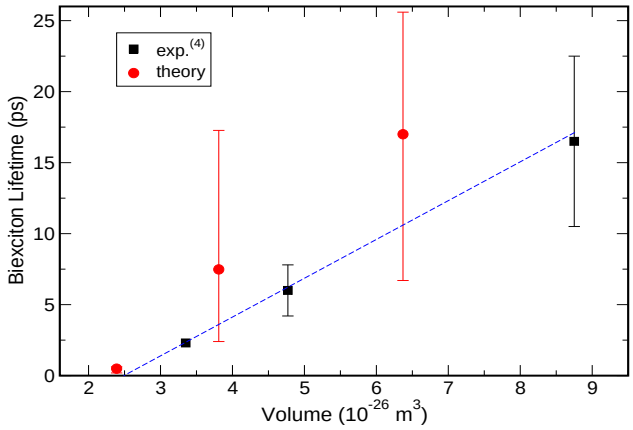

Figure 4: Biexciton recombination times as a function of dot volume: comparison of our results (red solid circles) with experiment[4] (black solid squares). The dashed line is a linear fit through the experimental data.

band edge states are optically allowed. Interestingly, even an atomistic approach like tight-binding fails to predict the correct behavior of the excitonic gap in CQDs with diameters > 5 nm, perhaps owing to a too restricted choice of the basis set used,[20] which may limit the validity of the electronic structure description to regions near the Γ point.

We now turn to the important issue of determining the origin of the observed peculiar lifetimes of non-radiative carrier dynamics. Non-radiative biexciton decay is generally attributed in CQDs to efficient Auger recombination (AR), in which the energy of an electron-hole pair is non-radiatively transferred, upon recombination, to one of the remaining charge carriers, resulting in the transition from a ground state biexciton to a hot exciton.[6] This is the inverse of carrier multiplication, a process whose importance in photovoltaics has been repeatedly emphasized,[9,22] where two electron-hole pairs are generated upon the absorption of a single, high-energy photon.[23] Observed AR times in CdSe CQDs ranged from 45 ps to 147 ps for dots with radii between 2.3 nm and 2.8 nm[6] (i.e., V=5.1$\div$9.2 10^{-26} m^3). In contrast, the biexciton decay times measured in InSb dots (6 ps to 16.5 ps for V$\sim 4.8 \div 8.8\ 10^{-26}$ m^3,[4] corresponding to R$\sim 2.25 \div 2.75$ nm), although scaling linearly with the nanostructure volume, as expected for AR,[5,6] were about 1 order of magnitude smaller than in CdSe[6] and PbSe (50 ps for R$\sim$ 2.4 nm[24]), and about a

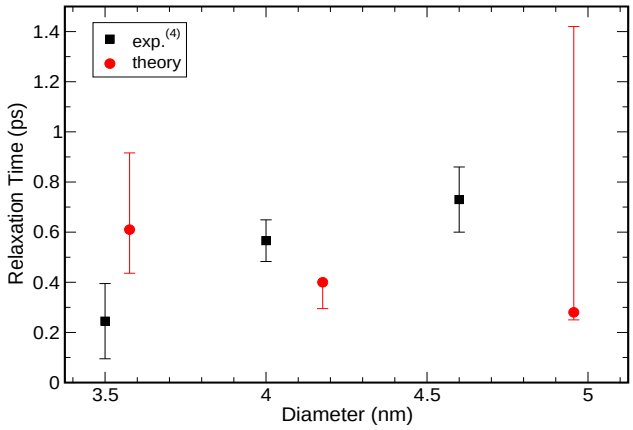

Figure 5: Electron cooling times as a function of dot diameter: comparison of our results (red solid circles) with experiment[4] (black solid squares). For details on the determination of the error bars on the theoretical data see text and Fig. S1 (Supporting Information).

factor of 2 faster than AR times observed in InAs CQDs[9] ($\sim$ 10 ps for V=4.0 10^{-26} m^3). If these exceptionally fast biexciton decay times were indeed due to AR, then they could hint to very efficient carrier multiplication in these systems, as the two processes share the same matrix elements. This, coupled with a small electron effective mass, a low band gap and the highest mobilities among semiconductor materials, would make InSb CQDs ideal building blocks for next-generation solar cells.

Aiming to shed light on this issue, we therefore calculated AR times for oleic-acid-capped InSb dots in tetrachloroethylene[4,25] with three different radii in the experimental range. Our results for $R = 2.1$ nm are shown in Fig. S1 (Supporting Information), where τ_{XX} is plotted as a function of ΔE_g, the variation of the energy gap around the value calculated for this size ($\Delta E_g = 0$), for a range of energies corresponding to a 5% size distribution. As in previous studies,[8] the AR times display some oscillations with ΔE_g, as the energies of initial and final states move in and out of resonance (see (1)). In order to capture this feature, in comparing our results with experimental data in Figure 4 we assign to each dot size the AR time calculated at $\Delta E_g = 0$, with (generally asymmetric) error bars equal to the largest variations of τ_{XX} in an energy interval corresponding to a $\sim$ 5% size distribution (see the thin black arrows in Fig. S1). The results presented in Figure 4 con-

firm that the biexciton decay times measured experimentally are indeed due to efficient AR, opening the door for the exploitation of these nanostructures in photovoltaics.

Interestingly we find that AR times calculated for InAs and InSb dots of similar sizes ($R = 2.0$ nm vs $R = 2.1$ nm, respectively) in similar conditions (i.e., with the same capping agents and in the same solution[25]), have similar magnitudes (i.e., they are the same within the estimated error bars - compare red and green curves and red and green symbols in Fig. S1). The difference observed experimentally[4,9] may therefore be attributable to surface and environmental effects.

Comparison between wurtzite CdSe dots with $R = 1.92$ nm and InSb dots with $R = 1.78$ nm, shows that the faster biexciton decay observed in the latter system may be attributed to a combination of different factors: (i) the material's crystal structure and (ii) the small band gap of InSb. (i) Compared to the single excitation channel available, upon non-radiative recombination of a ground state electron-hole pair, to the remaining band edge charge carriers in wurtzite materials [$|e_1,e_1;h_1\rangle \rightarrow |e_n\rangle$ for the electron and $|e_1;h_1,h_1\rangle \rightarrow |h_n\rangle$ for the hole, see (2)], the two-fold degeneracy of the valence band maximum in zincblende materials provides twice as many channels for the electron excitation [i.e., $|e_1,e_1;h_1\rangle \rightarrow |e_n\rangle$ and $|e_1,e_1;h_2\rangle \rightarrow |e_n\rangle$], and three times as many for the hole excitation process [i.e., $|e_1;h_1,h_1\rangle \rightarrow |h_n\rangle$, $|e_1;h_1,h_2\rangle \rightarrow |h_n\rangle$ and $|e_1;h_2,h_2\rangle \rightarrow |h_n\rangle$]. (ii) Auger coupling for the hole excitation process is found to be over two orders of magnitude stronger in InSb (where it represents the most efficient decay) than in CdSe (where, in contrast, τ_e is nearly a factor of 4 faster than τ_h, see (2)); the calculated AR matrix elements for the electron excitation process are instead only a factor of ~ 6 larger in InSb. We suggest the larger AR coupling to be a consequence of the smaller band gap of InSb, leading to a larger overlap in this material, compared to CdSe, between the (final) excited states involved in AR (which are located $\sim E_g$ away from the band edges and have therefore a higher kinetic energy and, likely, a higher charge density close to the dot surface in CdSe than in InSb) and the (initial) band edge states (which are more localized within the

core). These arguments are supported by the fact that InAs CQDs, which have bandgaps similar to InSb dots of the same size, and share the same crystal structure, also exhibit similar calculated AR times.

Fast, but not unusual, electron intra-band decay times were also reported recently in InSb CQDs[4] and attributed to Auger cooling (AC), a non-radiative decay process in which the excess energy of a hot electron is transferred, upon its decay to the conduction band edge, to the hole, which is excited deep in the valence band.[6] Our calculated AC times are in agreement with experiment, as shown in Figure 5 (where the error bars have been obtained following a similar procedure as in Figure 4), confirming that both non-radiative decay processes observed in this material are Auger-like.

In summary, the application of the atomistic semiempirical pseudopotential method to InSb CQDs has evidenced: (i) the s-like symmetry of their VBM in both In-rich and Sb-rich structures, in contrast with the predictions of less sophisticated approaches; (ii) a non-monotonic behavior of the L-component (i.e., the contribution from k-vectors close to the L point in the Brillouin zone) of the CBM wave function with size, in Sb-centered structures (not exhibited by In-centered CQDs), leading to (iii) an apparent failure of the band edge absorption to converge to the bulk band gap, even for considerably large dot sizes, consistent with observation, as the transition to a completely Γ-like CBM, and therefore a bulk-like band edge absorption, is expected to occur at a size close to the exciton Bohr radius; (iv) the importance of the structure's stoichiometry as a crucial input in the calculations, as only considering the observed composition will lead to an accurate reproduction of the experimental data for both radiative and non-radiative decay processes; (v) the unsuitability of continuum-like approaches to model InSb CQDs, as they lack the necessary atomistic detail to capture (a) the crucial difference between Sb-rich and In-rich structures of the same size, and (b) the details of the band structure away from Γ; (vi) the Auger-like nature of the extremely fast biexciton decay, that suggests the possibility of intriguingly high carrier multiplication yields in this system.

Acknowledgement

M.C. gratefully acknowledges financial support from the Royal Society under the URF scheme. A.S.'s work was supported by a DTG from the EPSRC.

Supporting Information Available

Plot of τ_{XX} vs ΔE_g for InSb and InAs CQDs with $R \sim 2$ nm. This material is available free of charge via the Internet at `http://pubs.acs.org`.

References

(1) Group IV, Elements, IV-IV and III-V Compounds. Part b - Electronic, Transport, Optical and Other Properties. In *Landolt- BoÌĺrnstein - Group III Condensed Matter*, Madelung, O.; RoÌĺssler, U.; Schulz, M., Eds.; Springer-Verlag: Germany, 2002; Vol. 41A1b.

(2) Liu, W.; Chang, A. Y.; Schaller, R. D.; Talapin, D. V. Colloidal InSb Nanocrystals. *J. Am. Chem. Soc.* **2012**, *134* 20258-20261.

(3) Luo, J.-W.; Franceschetti, A.; Zunger, A. Quantum-size-induced electronic transitions in quantum dots: Indirect band-gap GaAs. *Phys. Rev. B* **2008**, *78*, 035306.

(4) Chang, A. Y.; Liu, W.; Talapin, D. V.; Schaller, R. D. Carrier Dynamics in Highly Quantum-Confined, Colloidal Indium Antimonide Nanocrystals. *ACS Nano* **2014**, *8*, 8513-8519.

(5) Klimov, V. I.; Mikhailovsky, A. A.; McBranch, D. W.; Leatherdale, C. A.; Bawendi, M. G. Quantization of Multiparticle Auger Rates in Semiconductor Quantum Dots. *Science* **2000**, *287*, 1011-1013.

(6) Klimov, V. I. Optical Nonlinearities and Ultrafast Carrier Dynamics in Semiconductor Nanocrystals. *J. Phys. Chem. B* **2000**, *104*, 6112-6123.

(7) Pandey, A.; Guyot-Sionnest, P. Multicarrier Recombination in Colloidal Quantum Dots. *J. Chem. Phys.* **2007**, *127*, 111104-1-111104-4.

(8) Wang, L.-W.; Califano, M.; Zunger, A.; Franceschetti, A. Pseudopotential Theory of Auger Processes in CdSe Quantum Dots. *Phys. Rev. Lett.* **2003**, *91*, 056404.

(9) Schaller, R. D.; Pietryga, J. M.; Klimov, V. I. Carrier Multiplication in InAs Nanocrystal Quantum Dots with an Onset Defined by the Energy Conservation Limit. *Nano Lett.* **2007**, *7*, 3469-3476.

(10) Guyot-Sionnest, P.; Shim, M.; Matranga, C.; Hines, M. Intraband Relaxation in CdSe Quantum Dots. *Phys. Rev. B* **1999**, *60*, R2181-R2184.

(11) Kambhampati, P. Hot Exciton Relaxation Dynamics In Semiconductor Quantum Dots: Radiationless Transitions on the Nanoscale. *J. Phys. Chem. C* **2011**, *115*, 22089-22109.

(12) Califano, M. Direct and Inverse Auger Processes in InAs Nanocrystals: Can the Decay Signature of a Trion Be Mistaken for Carrier Multiplication? *ACS Nano* **2009**, *3*, 2706-2714.

(13) Wang, T.; Vaxemburg, R.; Liu, W.; Rupich, S. M.; Lifshitz, E.; Efros, Al. L.; Talapin, D. V.; Sibener, S. J. Size-Dependent Energy Levels of InSb Quantum Dots Measured by Scanning Tunneling Spectroscopy. *ACS Nano* **2015**, *9*, 725-732.

(14) Wang, L.-W.; Zunger, A. Local-Density-Derived Semiempirical Pseudopotentials. *Phys. Rev. B* **1995**, *51*, 17 398.

(15) Kim, D.; Kim, D.-H.; Lee, J.-H.; Grossman J. C. Impact of Stoichiometry on the Electronic Structure of PbS Quantum Dots. *Phys. Rev. Lett.* **2013**, *110*, 196802.

(16) Efros, A. L.; Rosen, M. Quantum Size Level Structure of Narrow-Gap Semiconductor Nanocrystals: Effect of Band Coupling. *Phys. Rev. B* **1998**, *58*, 7120-7135.

(17) At $D = 6$ nm the dots are almost stoichiometric with the number of In atoms in the cation-centered structures, however, lower than that of Sb atoms by 27 atoms out of a total of 3181, and *vice versa* for the anion-centered structures.

(18) Kilina, S.; Ivanov, S.; Tretiak, S. Effect of Surface Ligands on Optical and Electronic Spectra of Semiconductor Nanoclusters. *J. Am. Chem. Soc.* **2009**, *131*, 7717-7726.

(19) Franceschetti, A.; Fu, H.; Wang, L.-W. & Zunger, A. Many-body pseudopotential theory of excitons in InP and CdSe quantum dots. *Phys. Rev. B* **1999**, *60*, 1819-1829.

(20) Sukkabot, W. Tight-Binding Theory of the Excitonic States in Colloidal InSb Structures. *Mater. Sci. Semicond. Process.* **2014**, *27*, 51-55.

(21) Aurenhammer, F. Voronoi Diagrams âĂŞ A Survey of a Fundamental Geometric Data Structure. *ACM Computing Surveys* **1991**, *23*, 345âĂŞ405; Okabe, A.; Boots, B.; Sugihara, K.; Chiu, S. N. *Spatial Tessellations âĂŞ Concepts and Applications of Voronoi Diagrams*. 2nd edition. John Wiley, 2000, ISBN 0-471-98635-6; Tran, Q.T.; Tainar, D.; Safar, M. *Transactions on Large-Scale Data- and Knowledge-Centered Systems*, **2009**, ISBN 9783642037214.

(22) Semonin, O. E.; Luther, J. M.; Choi, S.; Chen, H.Y.; Gao, J.; Nozik, A. J.; Beard, M. C. Peak External Photocurrent Quantum Efficiency Exceeding 100% via MEG in a Quantum Dot Solar Cell. *Science* **2011**, *334*, 1530-1533; Padilha, L. A.; Stewart, J. T.; Sandberg, R. L.; Bae, W. K.; Koh, W.-K.; Pietryga, J. M.; Klimov, V. I. Carrier Multiplication in Semiconductor Nanocrystals: Influence of Size, Shape, and Composition. *Acc. Chem. Res.* **2013**, *46*, 1261-1269.

(23) Nozik, A. J. Quantum Dot Solar Cells.*Physica E* **2002**, *14*, 115.

(24) Schaller, R. D.; Petruska, M. A.; Klimov, V. I. Tunable Near-Infrared Optical Gain and Amplified Spontaneous Emission Using PbSe Nanocrystals. *J. Phys. Chem. B* **2003**, *107*, 13765-13768.

(25) The presence of specific capping agents and solutions is accounted for by the appropriate choice of the dielectric constant outside the dot,[8] in this case $\epsilon = 2.5$.